EVALUATION OF TRABECULAR BONE PROPERTIES USING ULTRASONIC SCANNER

LUCYNA CIEŚLIK, JERZY LITNIEWSKI,
MARCIN LEWANDOWSKI, ANDRZEJ NOWICKI

Department of Ultrasound
Institute of Fundamental Technological Research
Polish Academy of Sciences
ul. Pawińskiego 5B, PL-02-106 Warszawa, Poland
lcieslik@ippt.gov.pl

Signals scattered in trabecular bone contain information about properties of the bone structure. Evaluation of this properties may be essential for osteoporosis diagnosis and treatment monitoring because the standard densitometry does not provide complete information about the bone strength. It was previously demonstrated that using numerical model of backscattering in trabecular bone it is possible to estimate some microstructural characteristics of bone. Model predicts departures from the Rayleigh statistics of the scattered signal envelope depended on the scatterer physical parameters and its shape uniformity. This study concerns examination of trabecular bone (calcaneus) in vivo*. Ultrasonic bone scanner operating at frequency of 1,5 MHz was used to collect backscattered signals. Data were processed in order to obtain the statistical properties of the signal envelope and to compare them with histograms resulting from modeling. This study is an approach towards developing a tool for the investigation of scattering in trabecular bone that can potentially provide clinically useful information about bone strength and condition.*

INTRODUCTION

In the last 20 years the quantitative ultrasonic methods were introduced as alternative procedures to radiographic examinations of bone (Langton 1994, Laugier et al. 1994a, 1994b). These methods were based on sound transmission and enabled the determination of the frequency-dependent attenuation coefficient, called BUA (Broadband Ultrasonic Attenuation, $dBMHz^{-1}cm^{-1}$) as well as sound velocity – SOS (Speed Of Sound, ms^{-1}) for the bones that are easily accessible from the outside. Usefulness and applicability of these measurements for prediction of osteoporotic fractures of bones have been proved in long-term studies (Hans et al. 1996; Thomson et al. 1998). Results from many examinations

demonstrated that BUA coefficient is closely correlated with BMD (Bone Mineral Density) values, obtained by X-ray densitometry. However, evaluation of bone strength requires not only the knowledge about its density but also about its microscopic structure.

Ultrasonic examinations of soft tissues, based on the analysis of scattered ultrasonic signal were successfully applied to characterize and to differentiate the tissues (Bamber et al. 1981, Lizzi et al. 1986). Similarly, signals that have been scattered in trabecular bone contain the information about the properties of the bone structure. Therefore, the scattering-based ultrasonic methods potentially enable the assessment of microscopic structure of bone.

Many investigations have been focused on the measurements and calculations of the backscattering coefficient for trabecular bone and the dependency of that coefficient on frequency (Chafaí et al. 2000, Laugier at al. 1997, 2000, Padilla et al. 2003, Wear and Garra 1998, Wear 1999). It has been demonstrated that using the backscattering model it is possible to estimate some microstructural characteristics from experimental signals measured *in vitro* for calcaneal samples (Jenson et al. 2003, Pereira et al. 2004). Chaffaí et al. (2002) revealed a significant correlation between broadband ultrasonic backscatter (BUB) and the density and microstructure of the human calcaneus *in vitro*. Also, ability of ultrasound backscattering to predict mechanical properties of trabecular bone was shown by Hakulinen et al. (2004) who proved for the bovine bone samples that the integrated reflection coefficient (IRC) and BUB are highly linearly correlated with Young's modulus, ultimate strength and yield stress.

Theoretical studies of ultrasonic scattering by trabecular bone were performed by Wear (1999). The model of a bone, proposed by Wear, consisted of a random space-distribution of long identical cylinders with a diameter much smaller than the wavelength, aligned perpendicularly to the acoustic beam axis. Therefore the scattering by trabecular bone was modeled as scattering of a plane wave by elastic cylinders.

In our previous study (Litniewski et al. 2009) we have developed the simulation technique that enabled determination of the ultrasound signal received at the pulse-echo transducer surface after interrogation of cancellous bone. The simulation can be applied for different scattering models of a trabecular structure. Mimicking the bone structure similarly to Wear's model, by a random distribution of long elastic cylinders but allowing for variations of it's physical parameters we have found the departures from the Rayleigh statistics of the scattered signal instantaneous amplitude (envelope) as the variation of cylinders diameters increased (Litniewski 2007). The influence of the variation of mechanical properties of a bone tissue forming the trabeculae was not observed. The departure from the Rayleigh statistics could be expected as the effective amount of scatterers in resolution cell significantly depends on the scatterers uniformity. However, the frequency dependence of the power backscattered coefficients calculated using modeled signals differed from the published experimental results (Chaffaí et al. 2000). Whereas these results show the frequency exponent exceeding the value of 3 in the case of simulated results the dependence was below the cubic one.

We have also performed a study intended to compare the results obtained with the cylindrical model with the two semi-empirical scattering models of trabecular bone (Litniewski et al. 2010) putting emphasis on their abilities to mimic the frequency dependent backscattering coefficient measured in the cancellous bone. In the simulation of the bone RF echoes the real properties of the bone and experimental conditions were taken into account. Three types of trabeculae mimicking scatterers were considered. First the bone consisted of cylinders with varying thickness (Gamma distributed) within the population, was assumed. The next two cases accounted for the contribution of thick and thin trabeculae to the total backscattered signal. The second model assumed existence of two populations of the cylindrical scatterers significantly differing in the average value of Gamma distributed

diameters (Fig.1 A). Finally, the mixed model composed of thick and thin trabeculae modeled respectively by cylindrical and spherical scatterers was examined (Fig.1 B). The last selection resulted from the similarity found between scattering on small sphere and finite cylinder. Calculated echoes demonstrated the usefulness of the mixed model. Frequency dependence of backscattering coefficient agreed well with the experimentally determined dependences. When the spherical scatterer was used to describe thin trabecula (mixed model) the exponents *(n*) of the power-law function fitting the frequency dependence of backscattering coefficient increased to the value exceeding 3. For the smallest of the concerned spherical scatterers, outnumbering three times an amount of thick cylindrical trabeculae the value of *n* equal to 3.853 was achieved.

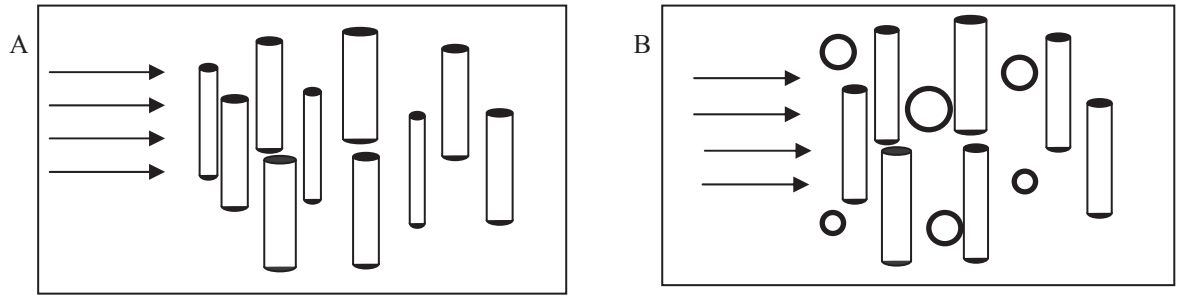

Fig.1. Trabecular bone model consisting of two populations of cylindrical scatterers (A) and bone model consisting of two populations of cylindrical and spherical scatterers (B). Arrows show the incidence direction of ultrasonic wave

The study also showed that the amplitude histograms calculated using demodulated RF echoes deviate from the Rayleigh distribution when the variation of scatterers' diameters increase. The simulations results demonstrated that the physical dimensions, such as size and shape of the individual scatterers, exerted influence on frequency dependence and on the statistics of scattered signals. The importance of thin interconnecting trabeculae in the bone structure model was demonstrated.

In this paper we show experimental results. Using the bone scanner the signals backscattered in the heel bone were collected and processed in order to determine the statistical properties of the signals envelopes. These results are compared with the modeling data.

1. MATERIALS AND METHODS

1.1 TRABECULAR BONE STRUCTURE

Trabecular (cancellous) bone (Fig.2) is one of the two types of osseous tissue (Myśliwski, 2007). It is less dense, softer, weaker, and less stiff in compare to the compact bone, which is the other type of osseous tissue. The primary anatomical and functional unit of trabecular bone is the trabecula (Fig.2 A) – the tiny lattice-shaped rod or plate that form the tissue structure. Trabecular bone is highly vascular and frequently contains fat cells (Fig.2 B) and red or yellow bone marrow (Fig.2 C) (Myśliwski, 2007). Because of a large surface area the trabecular bone is ideal for metabolic activity e.g. exchange of calcium ions. In osteoporosis, cancellous bone is more severely affected than cortical bone. The trabecular bone typically occurs at the ends of long bones, proximal to joints and within the interior of

vertebrae. Only calcaneus (the heel bone) may be easily examined *in vivo* because of its accessibility.

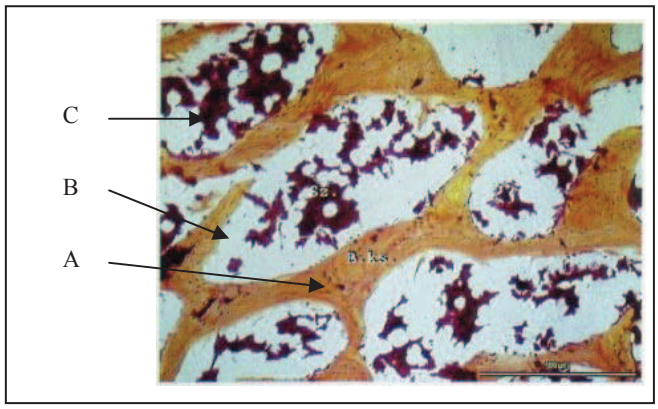

Fig.2. Histological slide of decalcified trabecular bone (Schmorl stain, zoom 40x). Trabeculae are basic structural units (A, orange). Between them bone marrow (C, purple) and fat cells (B, white) are located (Myśliwski *et all*., 2002)

1.2 ULTRASONIC SCANNER AND DATA ACQUISITION

Experimental measurements were performed using ultrasonic scanner (Fig.3 A) that was developed in our department. It provides sector scanning with the image frame rate up to 6 Hz. The scanner enables transmission of short sinusoidal signals at frequencies of 1,0 MHz, 1,5 MHz and 1,7 MHz. It is also possible to change transmitted signal duration and its shape. Scattered echoes are sampled at 20 MHz frequency with 11 bits resolution. Scanner is equipped with Time Gain Control (TGC) and received signal adjustable attenuator. In this study we have used a spherical transducer (with 15 mm diameter, 45 mm focal length). The received sequences were online envelope detected and displayed on the screen (Fig.3 B). Chosen RF data were stored separately and a file containing TGC information was saved as well.

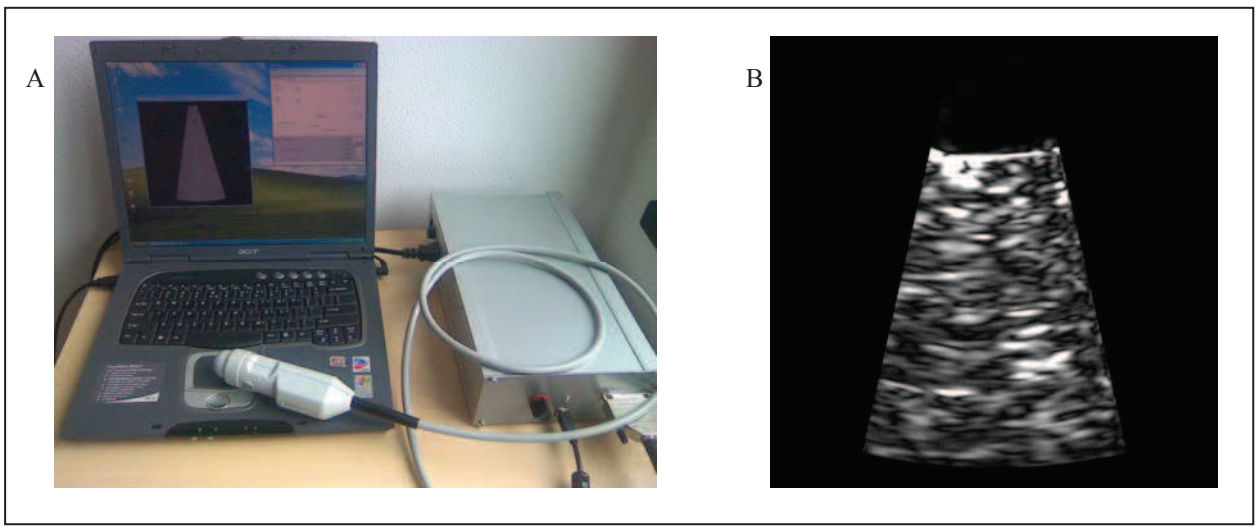

Fig.3. Ultrasonic scanner (A) and exemplary B-scan of trabecular bone *in vivo* (B)

In this study the bone was interrogated with one period long sinusoidal signals transmitted at driving frequency of 1,5 MHz. The measurements of calcaneus through lateral and medial surface were performed on both legs. Three healthy volunteers (age about 28) participated in this experiment.

1.3 SIGNAL PROCESSING

The aim of this study was to perform measurements *in vivo* and to show echo-envelope statistics in comparison to the previously calculated simulation data. To obtain reliable results it is necessary to take into account effects that influence signal amplitude and frequency contents and perform adequate operations to neutralize this influence. Signal processing included compensation of focusing, Time Gain Control (TGC) and attenuation. After data processing statistic calculations were performed.

Time Gain Control compensation

The level of TGC which was used during echo recording was stored in separate file. Thanks this, generation of gain curve was possible. It illustrates the gain level for each sample of echo signal (Nowicki, 2003). Next, the correction curve that compensated TGC was calculated. Because for each particular B-scan the different TGC conditions were applied the respective correction curves were calculated for each RF data set.

Focusing compensation

The considered signals were emitted from focused source. Focal distance depends on frequency. For higher frequencies the distance is shorter and for lower frequency waves it is longer. Thus, the pulse amplitude of high frequency component increases faster than amplitude of lower frequencies and as the consequence the pulse frequency contents changes. Thus it is necessary to compensate this effect before the attenuation coefficient estimation. Otherwise, in regions in front of the focus the attenuation is underestimated and in regions behind the focus it is overestimated.

In this work the effect of diffraction or focusing was compensated using amplitude spectrum of echoes obtained from a rigid plane reflector located in water perpendicularly to transducer axis at the various axial distances from the source. For each spectral component the correction that compensated the amplitude was calculated. Consequently the attenuation coefficient was then computed using the corrected power spectra.

Attenuation compensation

Attenuation coefficient used to attenuation compensation was obtained for each B-scan separately. The attenuation coefficient $\alpha_0(f)$ was determined using the spectral difference technique based on a comparison of the power spectrum of the backscattered signals recorded before and after propagation through the defined section of the medium. The following procedures were used.

First selected part of the scattered signal of the duration T was divided into N short partial signals A_i. These signals were separated by the distance Δt (Litniewski, 2006):

$$\Delta t = \frac{T - t_0}{N} \tag{1}$$

where t_0 is Gaussian window length used for A_i signals determination. This size was equal to 1,5 pulse duration.

Afterwards the spectra of A_i signals $|F(A_i)|$ were calculated by fast Fourier transform and partial attenuation coefficients $\alpha_i(f)$ were determined from the formula (Litniewski, 2006):

$$\alpha_i(f) = \frac{-\ln\left(\frac{|F(A_{i+1})|}{|F(A_i)|}\right)}{\Delta t \cdot v} \tag{2}$$

where v is the phase velocity of the longitudinal acoustic wave.

Finally average attenuation coefficient was calculated using following equation:

$$\alpha_0(f) = \frac{1}{N}\sum_N \alpha_i \tag{3}$$

The following algorithm for the compensation of attenuation was applied. First, the spectrum of attenuated signal FA was calculated. Next, the synthesis of a new signal F on the basis of spectral components of the backscattered signal was performed. During the synthesis, the amplitudes of spectral components were increasing with the increasing value of the depth co-ordinate corresponding to the penetration depth and the value of frequency-dependant attenuation coefficient α_{0k}. The process is described (Litniewski, 2006) by the formula:

$$F(t_i) = \sum_{k=1}^{M} FA_k \exp(\alpha_{0k} \cdot f_k \cdot v \cdot t_i) \exp(-2\pi j \cdot f_k \cdot t_i) \tag{4}$$

where k stands for the index of the spectral component, f_k denotes frequency, FA_k is a complex spectrum of backscattered signal, v denotes phase velocity of the longitudinal acoustic wave and α_{0k} is the frequency-dependant attenuation coefficient. $t_i = i \cdot \delta t$ stands for time, where δt is a time step given by the signal sampling rate. The summation is carried over the whole range of frequencies of backscattered signal. The real part of F is the desired backscattered signal compensated for attenuation.

Fig.4 shows raw RF signals before processing and compensated line after signal processing which involves: focussing, TGC and attenuation compensation.

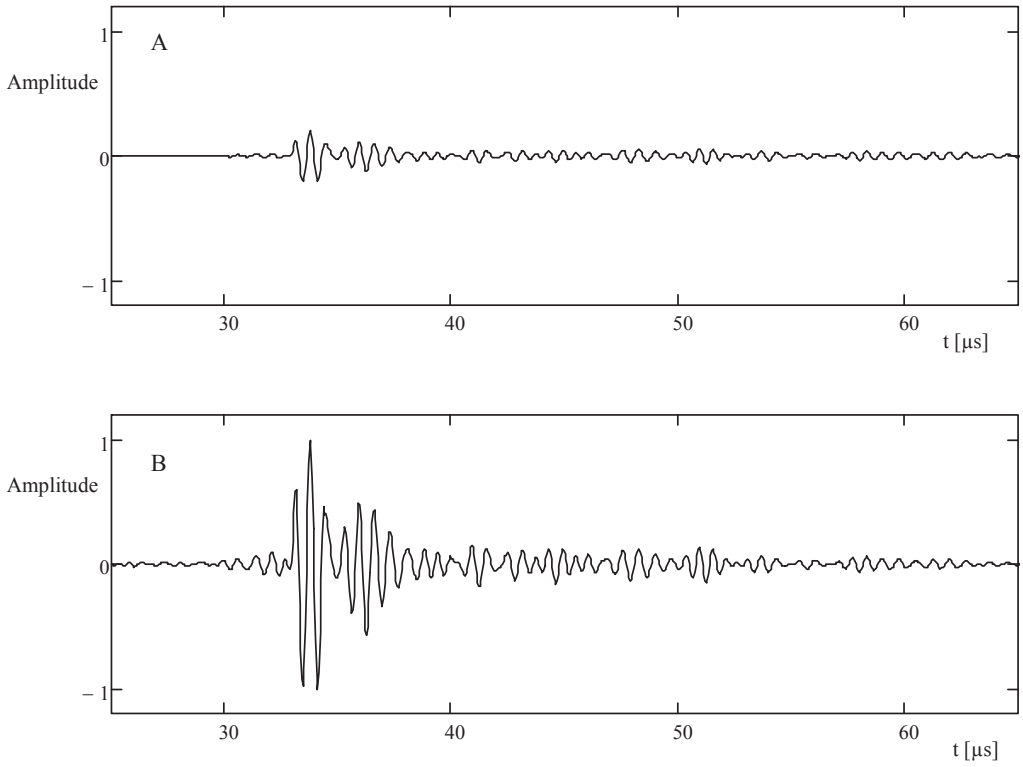

Fig.4. Raw RF signal (A) and processed (B) RF signal (compensated for focusing, TGC and attenuation)

1.4 STATISTICS DETERMINATION

The selection of the part of scattered signal intended for farther processing can not be done automatically because of anatomical differences of calcaneus and surrounding tissues. Thus the localization of trabecular bone scattering zone in respect to the first echo depends on soft tissue and compact bone thickness and the bone shape. The chosen signal part is derived by windowing the RF line with semi Gaussian window. Fig.5 presents processed RF signal (solid line) together with applied window (dashed line).

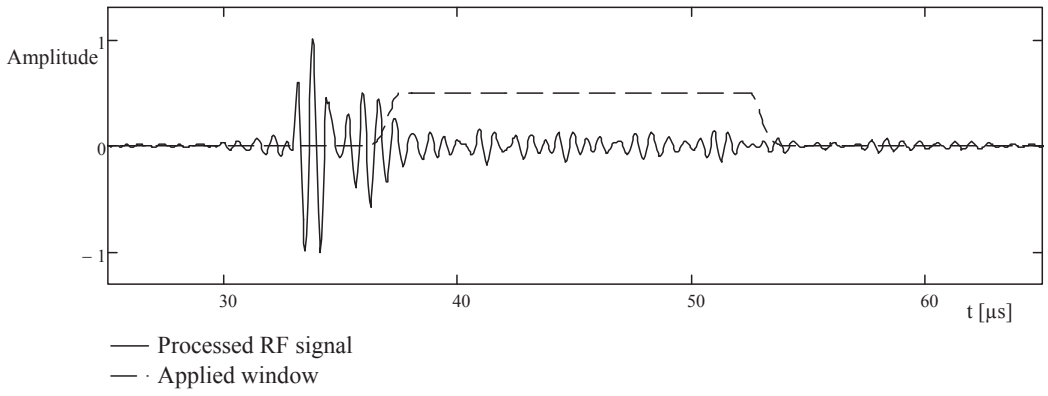

Fig.5. Processed RF signal and applied window

After the operations described in SIGNAL PROCESSING section and the selection of the trabecular bone scattering zone the magnitude of RF signal was calculated to obtain signal envelope. Fig.6 presents signal after focusing, TGC and attenuation compensation and its envelope.

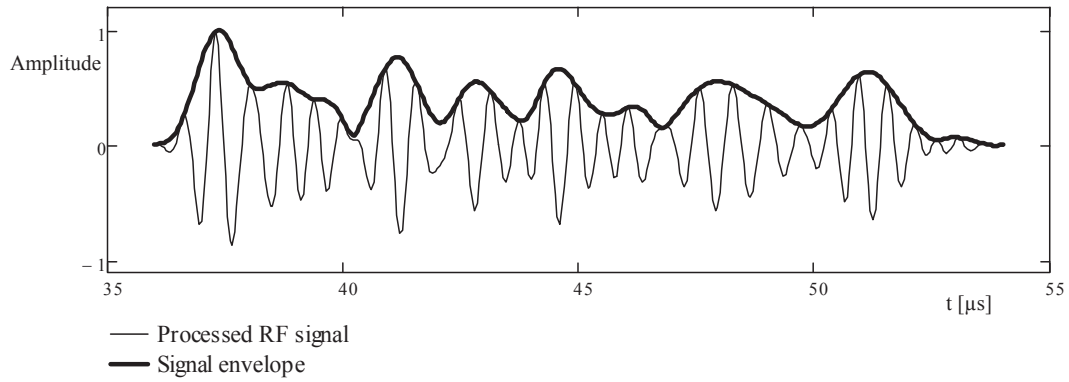

Fig.6. Processed RF signal (after focusing, TGC and attenuation compensations) and its envelope

To describe the variability of the signal envelope and of the trabeculae thickness the *MSD* (mean-to-standard deviation-ratio) coefficient was used. It is defined as (Balasundar and Mandayam, 2002):

$$MSD = \frac{\langle x \rangle}{\sigma} \tag{5}$$

where x is random variable, $\langle\ \rangle$ indicates the averaging operator and σ is standard deviation of variable x.

In this paper the envelope *MSD* coefficient was denoted as *eMSD* ($eMSD = \frac{\langle A \rangle}{\sigma(A)}$) and trabeculae thickness *MSD* as *tMSD* ($tMSD = \frac{\langle d \rangle}{\sigma(d)}$) where A and d stands respectively for the scattered signal amplitude and the scatterer diameter. The envelopes of the trabecular bone backscattered signals were used to calculate the envelopes mean value and standard deviation value and to determine the *eMSD* coefficient.

2. RESULTS AND DISCUSSION

Several studies shown (Mothlen et al. 1995, 1998) that the Rayleigh distribution describes well the statistics of backscattered signal envelope when the measuring volume contains a large number of randomly distributed scatterers. However the numerical calculations, presented in earlier studies demonstrated that the amplitude histograms

evaluated using demodulated RF echoes deviate from the Rayleigh distribution when the variation of scatterers' diameters increase (Litniewski et al. 2010).

As the Rayleigh distribution is characterized by mean-to-standard deviation-ratio (*MSD*) equal to 1,913 the *eMSD* values different than 1,913 were regarded as the departure from the Rayleigh statistics. In this chapter first the histograms of envelope values were presented and compared with theoretical Rayleigh distributions and next *eMSD* comparison of experimental and modeled results are discussed.

Statistics of *in vivo* measured acoustic data

In Fig.7 the histograms of compensated RF signal envelopes are shown together with calculated theoretical Rayleigh distributions. In each case the *eMSD* parameters were calculated and they are presented in Table 1.

Tab.1. The *eMSD* coefficient determined from the *in vivo* recorded data

Fig	**Volunteer**	**Leg**	**Surface**	***eMSD***
A	1	Right	Medial	1,797
B	1	Left	Medial	1,820
C	2	Left	Medial	1,673
D	2	Right	Lateral	1,881
E	3	Left	Lateral	1,706
F	3	Right	Lateral	1,867

All calculated *eMSD* coefficients are lower than the characteristic value for the Rayleigh distribution (1,913) and they vary from 1,673 to 1,881. But the differences are not significant except two cases (Table1. *eMSD* = 1.673 and 1.706). In case of these two results it can be assumed that the effective number of scatterers in the resolution cell is low what results in the departure from the Rayleigh statistics.

Comparison of the modeling results with the measured data

During the previous study three models mimicking the trabecular bone structure were developed, namely the one population cylindrical scatterers model, two population cylindrical model and two population model with mixed cylindrical and spherical scatterers (mixed model). Models accuracy was evaluated by verifying their ability to mimic the frequency dependent backscattering coefficient measured in the trabecular bone. The backscattering coefficient calculated using the mixed model was very similar to the experimental data when the frequency dependence was accounted. This model shows significant departure from the Rayleigh distribution of *eMSD* when the variation of trabeculea thickness increase (low *tMSD*).

Fig.8 A shows the predicted *eMSD* coefficient versus *tMSD* coefficient. In this figure results for three models are shown. The most pronounced changes were associated with the mixed model. For the assumed *tMSD* values varying form 1 to 4, the *eMSD* ranged from 1,44 to 1,89. For all models of bone starting from *tMSD* = 3, the *eMSD* values stabilized and were close to the value assigned to the Rayleigh distribution.

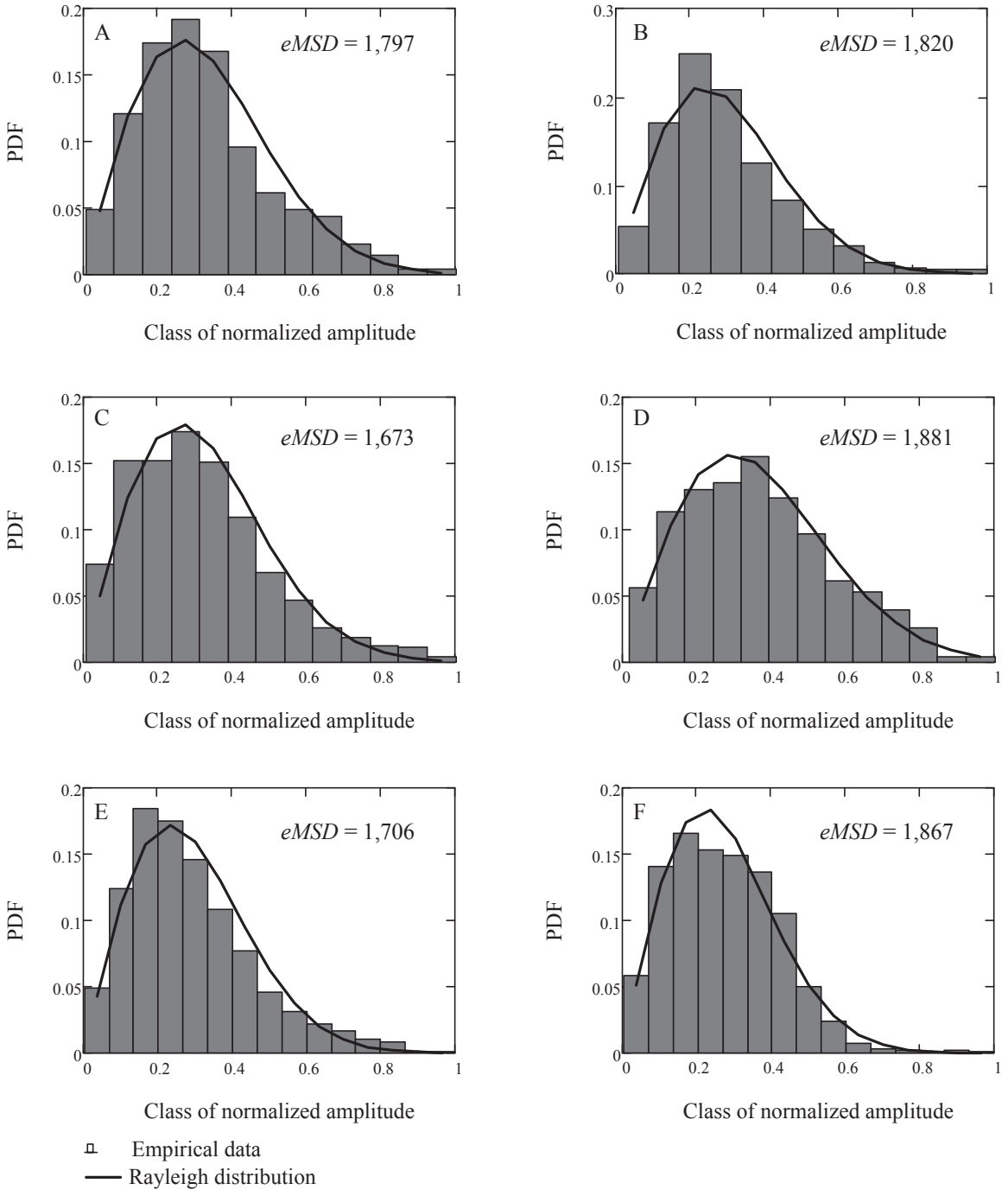

Fig.7. Exemplary histograms of processed RF signals envelops together with Rayleigh distributions

Also, the *eMSD* values obtained from *in vivo* signals present some variability ranging from 1,673 to 1,881. Fig.8 B presents maximum and minimum value of measured *eMSD* and the *eMSD* obtained assuming the mixed model. The range of the measured *eMSD* corresponds to the *tMSD* ranged from 1.3 to 4 as predicted from the mixed model of the trabecular bone. It is important to add that the typical values of *tMSD* measured in the trabecular bone samples varies between 1.7 and 12 (Hosokawa and Otani 1997, Kothari et al. 1999).

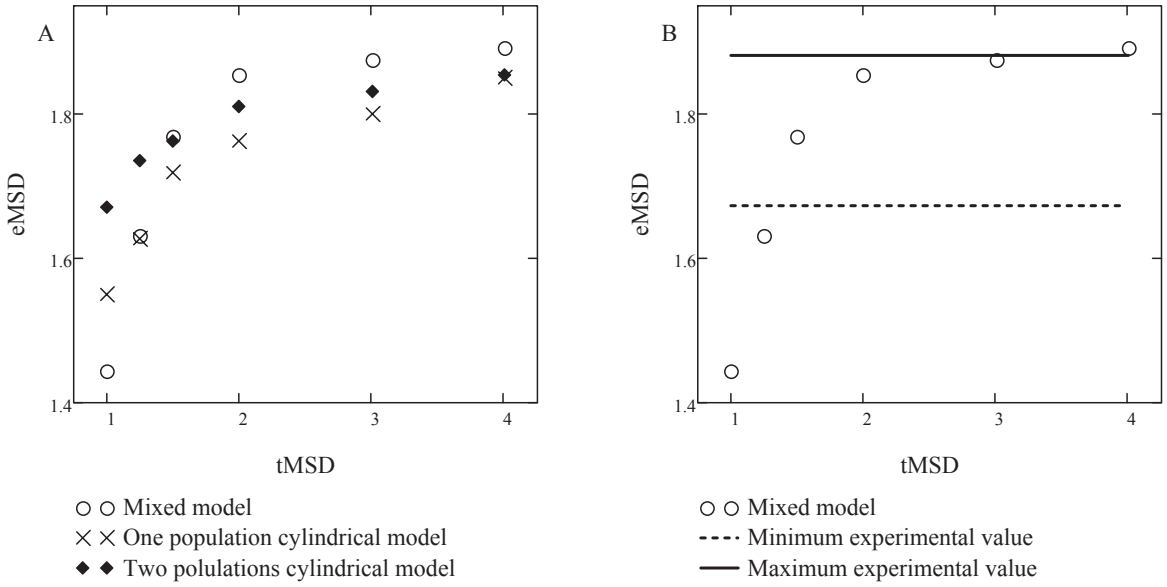

Fig.8. The *eMSD* coefficient versus *tMSD* coefficient calculated for 3 bone models (A) and mixed model results compared to experimentally obtained values (B)

3. CONCLUSIONS

The *eMSD* parameter of acoustic data collected *in vivo* from the heel bone was presented and compared to the numerically modeled predictions. It has been shown that:

(i) *eMSD* parameter of *in vivo* collected data varies form 1,673 to 1,881,

(ii) *eMSD* parameter of modeled data are in the range of *in vivo* values for the *tMSD* ranged from 1.3 to 4

(iii) the above-mentioned (ii) *tMSD* values are in the range of typical *tMSD*'s for the human trabecular bone

These preliminary *in vivo* obtained results are encouraging for the further modeling study. The simulation results presented in earlier studies demonstrates that the physical dimensions, such as size and shape of the individual scatterers influence the statistics of scattered signals. The experimental results presented above also show the cases of departure from the Rayleigh distribution. That indicates that the model proposed can potentially provide clinically useful information about bone condition and can be applied as a tool for the investigation of the ultrasound scattering in trabecular bone.

Further studies are necessary, including much bigger population, to assess the usefulness of the described and presented departures from the Rayleigh statistics for the evaluation of the trabecular bone condition.

ACKNOWLEDGEMENTS

Work supported in part by the Ministry of Science and Higher Education, Poland (N518388234).

LIST OF SYMBOLS

A	amplitude
A_i	short signal selected for attenuation calculations
d	scatterer diameter
$eMSD$	envelope mean-to-standard deviation-ratio
f	frequency
F	spectrum of a signal compensated for attenuation
FA	spectrum of attenuated signal
$\|F(A_i)\|$	spectrum of A_i signal
i	number of samples
j	imaginary unit
k	index of the spectral component
M	amount of spectral components
n	exponents of the power-law function
N	number of A_i signals
MSD	mean-to-standard deviation-ratio
$tMSD$	trabeculae mean-to-standard deviation-ratio
t_0	Gaussian window length
T	duration of a signal selected for attenuation calculations
v	phase velocity of the longitudinal acoustic wave
x	random variable
$\alpha_0(f)$	attenuation coefficient
$\alpha_i(f)$	partial attenuation coefficient
δt	time step given by the signal sampling rate
Δt	A_i signals distance
σ	standard deviation

REFERENCES

[1] J. Bamber, C. Hill, J. King, Acoustic properties of normal and cancerous human liver, Ultrasound in Medicine and Biology, Vol. l7, 121-133, 1981.

[2] B. I. Raju, M. A. Srinivasan, Statistics of Envelope of Hifg-Frequency Ultrasonic Backscatter from Human Skin In Vivo, IEEE Transactions on Ultrasonics, Ferroelectrics, and Frequency Control, Vol. 49, 871-882, 2002.

[3] S. Chaffaí, V. Roberjot, F. Peyrin, G. Berger, P. Laugier, Frequency dependence of ultrasonic backscattering in cancellous bone: Autocorrelation model and experimental results, Journal of the Acoustical Society of America, Vol. 108 (5), 2403-2411, 2000.

[4] S. Chaffaí, F. Peyrin, S. Nuzzo, R. Porcher, G. Berger, P. Laugier, Ultrasonic characterization of human cancellous bone using transmission and backscatter measurements: relationships to density and microstructure, Bone, Vol. 30 (1), 229-237, 2002.

[5] M. Hakulinen, J. Töyräs, S. Saarakkala, J. Hirvonen, H. Kröger, Ability of ultrasound backscattering to predict mechanical properties of bovine trabecular bone, Ultrasound in Medicine and Biology, Vol. 30 (7), 919-927, 2004.

[6] D. Hans, P. Dargent-Moline, A. Schott, J. Sebert, C. Cormier, P. Kotski, et al. Ultrasonographic heel measurements to predict hip fracture in elderly women: the Epidos prospective study, Lancet, Vol. 348 (9026), 511-514, 1996.
[7] A. Hosokawa, T. Otani, Ultrasonic wave propagation in bovine cancellous bone, Journal of the Acoustical Society of America, Vol. 101, 558-562, 1997.
[8] F. Jenson, F. Padilla, P. Laugier, Prediction of frequancy-dependent ultrasonic backscatter in cancellous bone using statistical weak scattering model, Ultrasound in Medicine and Biology, Vol. 29, 455-64, 2003.
[9] M. Kothari, T. Keaveny, J. Lin, D. Newitt, S. Majumdar, Measurement of intraspecimen variation in vertebral cancellous bone architecture, Bone, Vol. 25 (2), 245–250, 1999.
[10] C. Langton, The role of ultrasound in the assessment of osteoporosis, Clinical Rheumatology, Vol. 13 suppl. 1, 13-17, 1994.
[11] P. Laugier, P. Giat, G. Berger, New ultrasonic methods of quantitative assessment of bone status, European Journal of Ultrasound, Vol. 1, 23-38, 1994a.
[12] P. Laugier, P. Giat, G. Berger, Bone characterization with ultrasound: state of art and new proposal, Clinical Rheumatology, Vol. 13 suppl. 1, 22-32, 1994b.
[13] P. Laugier, P. Giat, C. Chappard, Ch. Roux, G. Berger, Clinical assessment of the backscatter coefficient in osteoporosis, 1997 IEEE Ultrasonic Symposium, 1101-1105, 1997.
[14] P. Laugier, F. Padilla, E. Camus, S. Chaffai, C. Chappard, F. Peyrin, M. Talmant, G. Berger, Quantitative ultrasound for Bone Status Assessment, IEEE Ultrasonic Symposium Proceedings, Vol. 2, 1341-1350, 2000.
[15] J. Litniewski, Wykorzystanie fal ultradźwiękowych do oceny zmian struktury kości gąbczastej, IPPT PAN, 113-117, Warszawa, 2006.
[16] J. Litniewski, Statistical Sensitivity of the Envelope of Pulse-Echo Signal Backscattered in Trabecular Bone: Simulation Study, 2007 International Congress on Acoustics, 6, 2007.
[17] J. Litniewski, A. Nowicki and P. A. Lewin, Semi-empirical bone model for determination of trabecular structure properties from backscattered ultrasound, Ultrasonics, Vol. 49, 505-513, 2009.
[18] J. Litniewski, A. Nowicki, J. Wojcik, Ultrasonic characterization of cancellous bone using three models of trabecular structure, Proceedings of 59th Meeting of Acoustical Society of America, 2010.
[19] F. L. Lizzi, M. Ostromogilsky, I. Feleppa, M. Rotke, M. Yaremko, Relationship of ultrasound spectral parameters to features of tissue microstructure, IEEE Transactions on Ultrasonics, Ferroelectrics, and Frequency Control, Vol. 33, 319-328, 1986.
[20] R. Molthen, P. Shankar, J. Reid, Characterization of ultrasonic B-scans using non-Rayleigh statistics, Ultrasound in Medicine and Biology, Vol. 21, 161-170, 1995.
[21] R. Molthen, P. Shankar, J. Reid, F. Forsberg, V. Narayanan, E. Halpern, C. Piccoli, B. Goldberg, Comparison of the Rayleigh and K-distribution models using *in vivo* breast and liver tissue, Ultrasound in Medicine and Biology, Vol. 24, 93-100, 1998.
[22] A. Myśliwski, P. Trzonowski, M. Okrój, Z. Dobrzańska, Atlas histologiczny, Wydawnictwo Pedagogiczne OPERON, 22, Gdańsk, 2002.
[23] A. Myśliwski, Podstawy cytofizjologii i histofizjologii, AMG, 87-89, Gdańsk, 2007.
[24] A. Nowicki, Wstęp do ultrasonografii, Podstawy fizyczne i instrumentacja, Medipage, 46-47, Warszawa, 2003.

[25] F. Padilla, F. Peyrin, P. Laugier, Prediction of backscattered coefficient in trabecular bones using a numerical model of tree-dimensional microstructure, Journal of the Acoustical Society of America, Vol. 113 (2), 1122-1129, 2003.
[26] W. Pereira, S. Bridal, A. Coron, P. Laugier, Singular spectrum analysis applied to backscattered ultrasound signals from in vitro human cancellous bone specimens, IEEE Transactions on Ultrasonics, Ferroelectrics, and Frequency Control, Vol. 51, 302-12, 2004.
[27] P. Thomson, J. Taylor, R. Oliver, A. Fisher, Quantitative ultrasound (QUS) of the heel predicts wrist and osteoporosis related fractures in women ages 45-75 years, Journal of Clinical Densitometry, Vol. 1, 219-225, 1998.
[28] K. Wear, B. Garra, Assessment of bone density using ultrasonic backscatter, Ultrasound in Medicine and Biology, Vol. 24 (5), 689-695, 1998.
[29] K. Wear, Frequency dependence of ultrasonic backscatter from human trabecular bone: Theory and experiment, Journal of the Acoustical Society of America, Vol. 106 (6), 3659-3664, 1999.